Endothelial network formation within human tissue-engineered skeletal muscle

D Gholobova[1,#], L Decroix[1,2,#], V Van Muylder[1], L Desender[1], M Gerard[1], G. Carpentier[3], H. Vandenburgh[4], L Thorrez[1,*]

[1] Tissue Engineering Lab, Department of Development and Regeneration, KU Leuven, E. Sabbelaan 53, 8500 Kortrijk, Belgium

[2] Current affiliation: Faculty of Physical Education and Physiotherapy, Department of Human Physiology and Sportsmedicine, Building L, Pleinlaan 2, 1050 Brussels, Belgium

[3] Laboratoire de Recherche sur la Croissance Cellulaire, la Réparation et la Régénération Tissulaires (CRRET), Faculté des Sciences et Technologie, Université Paris-Est, 94000 Créteil, France.

[4] Department of Pathology and Laboratory Medicine, Brown University, Providence, RI, USA

All work was performed in [1], except endothelial network analysis, which was performed in [3].

# These authors contributed equally and should be considered co-first authors

Author contact details:

Dacha Gholobova	email: dacha.gholobova@kuleuven.be	tel. +32 56 24 60 39
Lieselot Decroix	email: lotjedecroix@hotmail.com	tel. +32 56 24 60 39
Vicky Van Muylder	email: vicky.van.muylder@telenet.be	tel. +32 56 24 60 77
Linda Desender	email: linda.desender@kuleuven.be	tel. +32 56 24 60 77
Dr. Melanie Gerard	email: melanie.gerard@kuleuven.be	tel. +32 56 24 62 27
Dr. Gilles Carpentier	email: image.bio.methods@free.fr	tel. +33 14 5171454
Prof. Herman Vandenburgh	email: Herman_Vandenburgh@brown.edu	tel. +1 401 226 1252
Prof. Lieven Thorrez	email: lieven.thorrez@med.kuleuven.be	tel: +32 56 24 62 31

Fax: +32 56 24 69 94 (* Corresponding author)

Abstract

The size of *in vitro* engineered skeletal muscle tissue is limited due to the lack of a vascular network *in vitro*. In this paper, we report tissue engineered skeletal muscle consisting of human aligned myofibers with interspersed endothelial networks. We extend our bio-artificial muscle (BAM) model by co-culturing human muscle progenitor cells with human umbilical vein endothelial cells (HUVECs) in a fibrin extracellular matrix. First, the optimal medium conditions for co-culturing myoblasts with HUVECs were determined in a fusion assay. Endothelial growth medium proved the best compromise for the coculture, without affecting myoblast fusion index. Second, both cell types were cocultured in a BAM maintained under tension to stimulate myofiber alignment. We then tested different total cell numbers containing 50% HUVECs and found that BAMs with a total cell number of 2.10^6 resulted in well aligned and densely packed myofibers while allowing for improved interspersed endothelial network formation. Third, we compared different myoblast-HUVEC ratios. Including higher numbers of myoblasts improved endothelial network formation at lower total cell density, however improvement of network characteristics reached a plateau when 1.10^6 or more myoblasts were present. Finally, addition of Matrigel to the fibrin ECM did not enhance overall myofiber and endothelial network formation. Therefore, in our BAM model, we suggest the use of a fibrin extracellular matrix containing 2.10^6 cells of which 50-70% are muscle cells. Optimizing these co-culture conditions allows for a physiologically more relevant muscle model and paves the way towards engineering of larger *in vitro* muscle constructs.

Introduction

Skeletal muscle tissue has a capacity for self-renewal upon muscle injury, but when this is impaired, non-functional scar tissue replaces the damaged or lost muscle. Current therapeutic interventions include autologous muscle transpositions, but these are associated with donor-site morbidity and poor tissue survival and integration (1). As an alternative for autologous muscle transpositions, human skeletal muscle organoids can be created *in vitro* by tissue engineering. Next to potential applications in regenerative medicine, muscle organoids may also be used as an *in vitro* model for myogenesis or myopathology.

Culture and differentiation of myogenic progenitor cells on natural and synthetic biodegradable scaffolds (2,3) results in differentiated myofibers which are often unaligned. Parallel alignment of the myofibers can be induced when cells are subjected to a unidirectional force during differentiation and results in functional bio-artificial muscles (BAMs) which can be electrically and mechanically stimulated (4–6).

However, the size of *in vitro* created skeletal muscle tissue is limited due to the lack of a vascular network *in vitro*. Coculturing endothelial cells and myoblasts, muscle precursor cells, might overcome this problem. This way, the newly formed muscle can be prevascularized, meaning that an endothelial network is formed *in vitro* in the tissue engineered muscle. The goal is to anastomose this network to the host vasculature after transplantation. Although prevascularization of tissue engineered muscle has been described on scaffolds (7,8) , myofibers do not align in one direction on these scaffolds, precluding muscle contractility. Other tissue engineering approaches such as the use of soft hydrogels, the combination of endothelial cell sheets with myoblast cell sheets and microfabrication techniques such as 3D-printing may be more suitable to obtain aligned myofibers (7,9–13). Engineering muscle precursor cells in a soft hydrogel such as fibrin allows the myofibers to align in one direction while fibrin behaves pro-angiogenic, making it a good scaffold for both the formation of myofibers and endothelial networks.

Prevascularization of aligned tissue engineered muscle tissue has been described for murine muscle based on coculture of C2C12 murine myoblasts and embryonic heart endothelial cells (14). Another report describes the engineering of aligned, functional rat muscle with post-implantation vascular integration in mice (15). To our knowledge however, prevascularization of human aligned myofibers has not been described. In this work, we aimed to determine suitable culture conditions allowing both aligned myofiber formation and endothelial network formation as a first step towards a human vascularized BAM. Therefore, we used a coculture of human muscle cells, containing both myoblasts and fibroblasts, and human umbilical vein endothelial cells (HUVECs) in a fibrin extracellular matrix.

Methods

Cell culture. HUVECs labeled with Green Fluorescent Protein (GFP) (Angio-proteomie) were cultured on gelatin-coated culture flasks (0.1% gelatin, Millipore, pre-incubate for 1 hour at 37°C) in endothelial growth medium (EGM-2 with bullet kit, Lonza). GFP-HUVECs were split at 90% confluence and used in the experiment at passage 7. Human muscle cells (gift from H. Vandenburgh, Brown University, USA) were isolated by needle biopsy on a 27-year-old male volunteer from a muscle biopsy (vastus lateralis) according to procedures approved by the Institutional Clinical Review Board of the Miriam Hospital (Providence RI USA). They were cultured in Skeletal muscle Growth Medium (SkGM, Lonza), supplemented with 15% Fetal bovine serum (FBS, Lonza). Muscle cells were split at 60-70% confluence and used in experiments at 21 doublings.

3D tissue construct. Muscle cells and GFP-HUVECs were mixed with 500 µl thrombin (4 U/ml, Tissucol) and cast into 25-mm-long silicone rubber molds with end attachment sites. Then, 500 µl fibrinogen (2 mg/ml, Tissucol), with or without the addition of 20% Matrigel (BD Biosciences), was added and the cell-gel mix was mixed by quickly pipetting up and down, to form a fibrin gel (1 mg/ml, with or without 10% Matrigel) including both cell types. Following two hours incubation at 37°C, EGM-2 or SkGM medium supplemented with fibrinolysis inhibitors aprotinin (92.5 µg/ml Carl Roth) and tranexamic acid (400 µM, Sigma) was added and replaced every two days. For BAMs containing only muscle cells, the medium was switched to differentiation medium two days after casting (SkFM; DMEM with 10 ng/ml hEGF, 10 µg/ml insulin, 50 µg/ml BSA and 50 µg/ml gentamicin). BAMs were made with different cell type ratios and numbers. Medium was replaced every 2 days and BAMs were kept in culture for 7 days prior to thickness measurement and fixation.

Thickness measurements. Cross-sectional thickness of BAMs in culture was measured with a sterile micrometer at day 7 after casting.

Immunocytochemistry. Immunocytochemistry was performed in order to (i) determine the amount of myoblasts and fibroblast in the cell population and (ii) to characterize the fusion index of the

myoblasts. For desmin staining, muscle cells were cultured in SkGM in 12-well dishes for 2-3 days until 60-70% confluent. For determination of fusion index, the cells were cultured to 80% confluence in SkGM and then switched to SkFM for 4 days to induce fusion into myofibers. Fixation was performed in a 1:1 methanol-aceton mix at -20°C for 10 min. Next, cells were permeabilized in blocking buffer containing 0.2% Triton-X-100 (Sigma) and 1% bovine serum albumin (BSA, Sigma) in PBS (30 min, RT). Subsequently, cells were incubated for 2 hours (RT) with a monoclonal mouse antibody against desmin (Sigma, D1033, 1:200 in blocking buffer) or tropomyosin (Sigma, T9283, 1:100 in blocking buffer) to determine the myoblast percentage and the fusion index respectively. Cells were labeled with a polyclonal goat anti-mouse secondary antibody (Alexa Fluor 568, A11004, Invitrogen) for 30 minutes in the dark and subsequently incubated with DAPI (0.1 µg/ml in PBS, Life Technologies) for 1 hour. The percentage of myoblasts in a muscle cell population was defined as the ratio of desmin positive cells to the total amount of cells (identified by the DAPI-stained nuclei). Fusion index was defined as the ratio of tropomyosin positive cells to the total amount of myoblasts in the population.

Whole mount immunofluorescence staining and confocal microscopy. Constructs were washed (3x 15 min in PBS) and then removed from the attachment sites. Then, they were pinned on styrofoam to preserve their original shape while fixing in 4% formaldehyde (Merck) for 1 h and stored at 4°C in PBS. Immediately before whole-mount staining, samples were fixed a second time in -20°C methanol for 10 minutes and permeabilized in blocking buffer for 1 hour. Subsequently, BAMs were incubated overnight at 4°C with a monoclonal mouse antibody against tropomyosin (Sigma, T9283, 1:100 in blocking buffer). Next, BAMs were washed and incubated with a polyclonal goat anti-mouse secondary antibody (Alexa Fluor 568, A11004, Invitrogen, 1:200) for 30 minutes in the dark, followed by incubation with DAPI (Life Technologies, 0.1 µg/ml in PBS) for 1 hour. BAMs were stored in PBS in the dark until visualized.

Confocal imaging and data analysis. BAMs were placed on coverslips and visualized by confocal microscopy (Zeiss LSM710) within 48 hours. Per BAM, 5 z-stacks were acquired, each containing 20-40 images (depending on the intensity of the signal at various depths) every 5 µm towards the center of the BAM. For myofiber analysis, each 20 µm z-projection (image grouping performed by the ImageJ software (16)) was manually analyzed for different parameters of myofiber formation: myofiber alignment, length and diameter as well as number of myofibers per microscopic field. Myofiber alignment was determined by the standard deviation of the angles of the myofibers. A lower number thus indicates better alignment. For endothelial network analysis, each 60 µm z-projection was automatically analyzed by a customized version of the "Angiogenesis Analyzer", an ImageJ plugin created by Gilles Carpentier (17). This tool quantifies endothelial networks in an objective manner, by extracting characteristic information of the network. Parameters to define endothelial networks were: junctions (group of joined nodes, pixels with at least 3 neighbors), branches (elements delimited by a junction and one extremity), isolated segments (binary lines which are not branched), total length of endothelial network (interconnected segments, branches and isolated segments), % branching length (length of interconnected segments and branches divided by total network length) and meshes (areas enclosed by segments) (Figure S1).

Statistics. Number of replicates refers to number of analyzed images for microscopic analyses or to number of BAMs for thickness analyses. D'Agostino & Pearson normality test and Bartlett's test were used to verify normality of the data and equality of variances, respectively. Normally distributed data with equal variances were analyzed by an unpaired student t-test when two groups were compared. For comparing several normally distributed groups, a one-way ANOVA was used with a Bonferroni multiple comparison post test. For groups that were not normally distributed and/or had unequal variances, a non-parametric Mann-Whitney test was used for comparison between two groups while Kruskal-Wallis test followed by a Dunn's post test was performed for multiple comparisons. All values were expressed as mean ± standard deviation. * $p< 0.05$, ** $p< 0.01$, *** $p< 0.001$.

3. Results

3.1 Aligned myofibers are formed in fibrin BAMs cultured in EGM-2

We first characterized the cells expanded from human muscle biopsy. The myogenic progenitor population (further referred to as 'muscle cells') contained 92.1 ± 4.0% (n=15) myoblasts and 7.9 ± 4.0% fibroblasts as assessed by desmin staining. Myoblasts had a fusion index of 70.0 ± 5.7% (n=20) as determined by tropomyosin staining. To make BAMs, 1.10^6 of these cells were mixed in a fibrin ECM (1mg/ml) and cultured in growth medium (SkGM) for 2 days, followed by differentiation medium (SkFM) for 5 days. The cell-ECM mix contracted around 2 attachment sites and formed 2-cm long muscle organoids (Figure 1, inset) containing aligned myofibers (Figures 1A, 1B and 2A).

Aiming at the formation of endothelial networks and aligned myofibers in BAMs, cocultures of HUVECs and muscle cells were mixed in a fibrin ECM in a 50:50 ratio. They are further referred to as coculture BAMs, in contrast to regular BAMs that do not contain endothelial cells. To investigate if endothelial networks can be formed in these organoids, we first applied the same tissue-engineering procedure to cocultures of the muscle cells and endothelial cells. However, culturing 5.10^5 muscle cells and 5.10^5 GFP-HUVECs under these culture conditions resulted in poor survival of HUVECs as assessed by confocal fluorescence microscopy (data not shown). Since HUVECs are cultured in EGM-2 medium, muscle cell survival and proliferation in this medium was examined in 2D. Muscle cells proliferated in EGM-2, although significantly slower (doubling time 39.71 ± 1.59 hours, n=9) compared to SkGM medium (30.34 ± 0.55 hours, n=9). Optimal differentiation conditions for 2D cultures are obtained by growing the muscle cells for 2 – 3 days in SkGM until 80% confluency, followed by 3-4 days in SkFM (SkGM-SkFM). Performing the differentiation in EGM-2 medium for 5 days resulted in myofibers with significantly less nuclei per fiber (2.49 ± 0.10 nuclei per fiber, n= 29), compared to SkGM-SkFM differentiation (7.06 ± 0.58 nuclei per fiber, n=18). However, the fusion index does not differ significantly between EGM-2 (0.61 ± .012, n=29) and SkGM-SkFM (0.67 ± 0.01, n=18).

Next, we compared myofiber formation in the 3D organoid with 1.10^6 muscle cells cultured in EGM-2 medium versus SkGM-SkFM medium. Whole mount tropomyosin staining was performed to visualize the formation of myofibers. Multinucleated myofibers formed in both EGM-2 and SkGM-SkFM media. However, myofibers cultured in EGM-2 contained a significant lower number of nuclei per myofiber (2.29 ± 0.10, n=10) compared to those cultured in SkGM-SkFM (3.09 ± 0.15, n=10) (Figure 2). Culturing BAMs in EGM-2 also decreased the diameter of the formed myofibers. On the other hand, there was no significant difference between the use of the two media in the number and length of myofibers and the alignment factor (Table 1 columns A and D). Also, the total thickness of the fibrin BAMs with 1.10^6 muscle cells was similar in SkGM-SkFM (2.48 ± 0.224 mm, n=3) versus EGM-2 (2.76 ± 0.159 mm, n=3). Since EGM-2 allowed culturing of muscle cells and HUVECs with formation of myofibers while enabling an optimal survival of the HUVECs, we further optimized coculture BAMs in EGM-2 medium.

3.2 Formation of aligned myofibers and endothelial networks in fibrin BAMs with a coculture of muscle cells and HUVECs

Coculture BAMs with 50% endothelial cells were further studied in EGM-2 medium with different total cell numbers (Figure 3). The thickness of the BAM was inversely proportional with the total number of cells used, both in BAMs with and without HUVECs (Table 2 column A).

BAMs and coculture BAMS, containing the same number of muscle cells (5.10^5 or 1.10^6), showed similar myofiber formation and alignment (Table 1 columns B-C and D-E, Figure S2). Myofibers were better aligned and more densely packed in coculture BAMs with a higher total cell number of 2.10^6 versus 1.10^6 (Figure 3). Compared to coculture BAMs with a total number of 1.10^6, coculture BAMs with 2.10^6 cells showed a significant increase in myofiber density and alignment (Table 1 columns C and E, Figure S2, Video S1). We hypothesized that also endothelial network formation would be enhanced. Indeed, the endothelial networks were significantly improved in the coculture BAMs with 2.10^6 cells (Figure 4, Table 3 column A and D, Figure S3, Video S2). The presence of meshes was detected in coculture BAMs and confirms formation of extended endothelial networks (Figure 3, Figure 4).

3.3 30% HUVECs suffice to induce endothelial networks between aligned myofibers

Based on our previous findings and on research from other groups (7,9,18), we started experiments with coculture BAMs with a ratio of 50% muscle cells and 50% HUVECs to obtain myofiber and endothelial network formation. To optimize this ratio, BAMs with a total of 1.10^6 or 2.10^6 cells were made with different ratios, ranging from 50-70% muscle cells and 50-30% HUVECs.

In coculture BAMs with a total of 1.10^6 cells, a muscle cell:HUVEC ratio of 60:40 or 70:30 showed significant better endothelial network formation, compared to coculture BAMs with a 50:50 ratio (Table 3 columns A-C, Figure 4, Figure S3). Although there was a trend towards further improvement

of the endothelial network formation in the 70:30 ratio compared to the 60:40 ratio, this was not significantly different. In the condition with a high percentage of HUVECs (50%), dense clusters of HUVECs occurred at certain places on the surface of the BAMs, which could not be analyzed by Angiogenesis Analyzer. When a total number of 2.10^6 cells was used, all ratios performed equally well (Table 3 columns D-F). However, when compared with the same ratio in BAMs with 1.10^6 cells, there was a significant improvement in endothelial network formation for each ratio, indicating that increasing the total cell number to 2.10^6 is beneficial for all ratios studied (Video S2). The dense clusters of HUVECs mentioned above were not observed in BAMs with a total cell count of 2.10^6 cells.

In coculture BAMs with a total of 1.10^6 cells, a ratio of 60:40 or 70:30 also showed significant better myofiber formation, compared to coculture BAMs with a 50:50 ratio: there was a significant increase in myofiber density and alignment (Table 4 columns A-C, Figure S4). When a total cell number of 2.10^6 was used, no major changes towards improvement of myofiber formation could be detected with increasing ratios of myoblasts (Table 4 columns D-F, Figure S4). When comparing the same ratios in BAMs with 1.10^6 versus 2.10^6 cells, there only was a consistent improvement in alignment of myofibers for the BAMs with 2.10^6 cells.

3.4 Matrigel impacts myofiber distribution, but does not improve myofiber and endothelial network formation

In tissue engineering, Matrigel is often used as a (component of) hydrogel, because it contains a complex mixture of extracellular matrix components and growth factors and has a beneficial impact on tissue growth *in vitro* (1,14). We hypothesized that addition of Matrigel to the fibrin ECM might enhance myofiber and endothelial network formation.

We assessed the addition of 10% Matrigel to the ECM of fibrin. This did not significantly change the thickness of the BAMs, neither in BAMs with 1.10^6 muscle cells, neither in coculture BAMs with 5.10^5 muscle cells and 5.10^5 HUVECs (Table 2).

While in BAMs with 1.10^6 muscle cells in fibrin only, myofibers are evenly distributed throughout the BAM, the addition of 10% Matrigel to the ECM causes an uneven distribution and formation of myofibers. An outer region of 20-30 µm was observed, containing densely packed and highly aligned myofibers and a core with lower cell density containing significantly lower length and alignment of myofibers (Table 1, compare columns F - G with column D, Figure S5).

Compared to the homogenously distributed fibrin BAMs, the outer densely packed region shows significantly longer myofibers, but there is no significant difference in alignment, fiber diameter or number of myofibers (Table 1, column F versus D). The inner region contains myofibers that are less well aligned with no significant difference in the other parameters (Table 1, column G versus D). To conclude, the addition of 10% Matrigel does not result in a better myofiber formation throughout the entire BAM, but only in a small outer region of the BAM. In contrast, a decreased myofiber alignment is observed in the inner region. Overall, myofiber formation is heterogeneous throughout the BAM in the presence of Matrigel in the ECM.

Discussion

Obtaining thicker tissue engineered constructs is one of the important goals in the field of tissue engineering. In order to succeed, vascularization is essential for obtaining viable constructs with increased survival time *in vitro* and improved engraftment upon transplantation (7,9,18). To do this, networks of endothelial cells, which form the innermost layer of blood vessels, must be established within the tissue engineered muscle. The current BAM model consists of aligned multinucleated myofibers, without endothelial cells, starting from a population of human myoblasts and fibroblasts cast in ECM (19). We used the natural hydrogel fibrin as a scaffold for the cells rather than collagen or other alternatives. This choice was made because of its stiffness characteristics and angiogenic properties (20–24). The formation of 3D tissue engineered human muscle in a fibrin ECM was already described in detail before, however endothelial cells were not present in these 3D cultures (24). In our work, HUVECs were added to the muscle cell – fibrin mix to obtain endothelial networks between the myofibers. HUVECs are relatively easy to obtain from umbilical cord, are robust in culture and are capable of endothelial cell tube formation *in vitro* (25,26). Adding multiple cell types in an organoid presents a challenge regarding culture conditions (27). Also in our system, culture conditions needed to be modified to sustain growth and differentiation of both cell types. We observed that endothelial cells fail to survive and form networks in the optimal culture condition for fibrin BAMs in skeletal muscle growth and differentiation medium. Therefore, we analyzed myofiber formation in BAMs cultured in EGM-2, a growth medium optimized for endothelial cells. This resulted in thinner myofibers with fewer nuclei per fiber, compared to the original medium. This may be explained both by a decreased proliferation of myoblasts during the first 2 days in EGM-2 versus SkGM, resulting in a lower cell density and a decreased myoblast fusion in EGM-2 as observed by a lower number of nuclei per myofiber. Nevertheless, aligned myofibers were still formed in BAMs cultured in EGM-2 medium while allowing the survival of HUVECs, making it the preferred medium for sustaining coculture BAMs.

Next, we investigated varying total cell numbers per BAM and different ratios of HUVECs versus muscle cells to determine the impact on endothelial network formation as well as myofiber formation. For BAMs with 1.10^6 total cells and 50% HUVECs, limited branching and mesh formation was observed. Network characteristics could be improved in cocultures with 40 or even 30% HUVECS. These endothelial networks have a higher number of branches and junctions and a lower number of isolated segments compared to the 50% HUVEC BAMs. The biggest improvement however was observed when a total cell number of 2.10^6 was used instead of 1.10^6 (Video S2). In these BAMs, the total length of the endothelial network doubled, concurrent with a higher number of meshes, branches and junctions and a lower number of isolated segments. For 2.10^6 cells, there was no further improvement when the muscle cell:HUVEC ratio was increased from 50:50 to 60:40 or 70:30. This suggests that for the given system and conditions tested a maximal endothelial network formation was reached when 2.10^6 cells were used, independent of the muscle cell:HUVEC ratio. Also for myofiber formation, the 30% and 40% HUVEC BAMs with a total cell number of 1.10^6 contained a higher number of myofibers that were thicker and better aligned than in the 50% HUVEC BAMs. Moreover, in the 50% HUVEC BAMs, HUVECs were unequally distributed throughout the BAM with denser layers towards the surface. These dense layers of HUVECs were not observed in the conditions with 2.10^6 cells, pointing to a better distribution of the HUVECs within the BAM. Overall, parameters of myofiber formation performed equally well or better when using 2.10^6 cells versus 1.10^6 cells. Similar to endothelial network formation, changing the muscle cell:HUVEC ratio did not further influence myofiber formation for 2.10^6 total cells. These and the above findings suggest an optimal combination of myofiber and endothelial network formation in coculture BAMs with 2.10^6 cells and a minimum of 50% muscle cells (Video S3). The presence of 1.10^6 muscle cells (both in BAMs with or without endothelial cells) has a double advantage over BAMs with only 5.10^5 muscle cells. First, as can be expected when using more muscle cells, myofiber density is higher. Second, a concurrent positive effect is observed in the alignment of myofibers. At the tissue level, BAMs with a higher total cell number have a significantly smaller thickness, regardless of the type of cells. This

may be explained by an augmented cell-mediated contraction of the ECM. We can conclude that the presence of HUVECs does not impair the formation of myofibers.

In addition to a better endothelial network formation when doubling total cell number per BAM, an increased amount of muscle cells has an important effect on endothelial network formation in the presence of similar amounts of HUVECs (compare Table 4 column A vs column F). It has been described that VEGF is also produced by myoblasts and this expression is enhanced when myofibers are kept under uniaxial tension (14). In the experiments described in this paper, we used endothelial growth (EGM-2) medium, which contains 0.5 ng/ml VEGF. Addition of VEGF in constructs with only endothelial cells lead to a more organized growth pattern of the endothelial cells (14). Although the amount of VEGF secreted by the myofibers in the cell culture medium (< 0.3 ng/ml) (14) was much lower than the amount of VEGF present in EGM-2 medium, local VEGF concentrations in our extracellular fibrin matrix may be much higher because of VEGF binding to fibrin (28). This is consistent with the observation that even lower total amounts of HUVECs still result in better endothelial network formation when total cell number is kept at 1.10^6, since the total amount of myofibers is higher.

In none of the myofibers we visualized, we could detect cross-striations. These have been described *in vitro* both in 2D (29) as well as in 3D muscle cultures (30,31). We performed confocal microscopy at day 7 of cocultures, whereas cross-striations were reported only after 14 days of culture. Next to a prolonged culture time, supplementing EGM-2 medium with specific growth factors to stimulate myoblast fusion such as MAGIC-F1 protein, IGF-1 and follistatin (32), can be explored in the future. Also, subjecting BAMs to electrical and/or mechanical stimulation has been described to further improve several muscle characteristics such as viscoelastic properties, protein synthesis, myofiber diameter and density, thus improving the level of maturation of myofibers (33,34).

Next to HUVECs, other endothelial cell populations may be worthwhile further investigation. In particular, endothelial colony forming cells (ECFCs), also termed blood outgrowth endothelial cells

(BOECs), are able to perform *de novo* tube formation and are pro-angiogenic *in vitro* and *in vivo* (35). Human peripheral blood and umbilical cord blood ECFCs form *de novo* functional blood vessels when seeded into a matrix and implanted *in vivo* (36). Microvessel density was similar for ECFCs and HUVECs, indicating a robust vasculogenic potential for both cell types (37). Adult peripheral blood ECFCs formed unstable vessels, while umbilical cord blood derived ECFC transiently formed vessels when implanted alone and were stable for four months when co implanted with fibroblasts in an immunodeficient recipient (38). Our muscle cell population also contains fibroblasts. These have been described to provide support for endothelial cells as well as modulate their migration, viability, and network formation (39). Optimizing fibroblast ratios and/or using other cell populations such as pericytes to stabilize endothelial networks may also further improve the cocultures (40). It remains to be seen though if the type of endothelial cells which are used *in vitro* is a critical factor once the construct is implanted, since the implanted endothelial network may be replaced by the host. Engineered human vascular networks, which were transplanted into third-degree burns connected with the host vessels during the first week, but during a remodeling phase in the second week after transplantation, the transplanted vessels regressed (41) and were replaced by host vessels. Transformation into mature blood vessels occurs via an inflammation-mediated process of vascular remodeling (42).

As described by others (7,9,11,18), prevascularization of tissue engineered muscle improves vascularization, blood perfusion and survival of the muscle constructs upon transplantation. Specifically, Koffler and colleagues (18) have shown that the degree of prevascularization *in vitro*, which highly depends on ECM, cell types, cell number, culture conditions and duration of *in vitro* culture, determines the *in vivo* vascularization. The goal of our study was to optimize experimental conditions in order to obtain maximal endothelial network formation in coculture BAMs. These findings open perspectives towards culture of larger, prevascularized BAMs with potential for human muscle transplantations as well as a physiologically relevant *in vitro* model for studying diseases and therapies (5,43,44). Host blood vessels are able to invade avascular muscle bundles (45), however

this still limits the size of muscle bundles that can be kept in culture pre-implantation. Ideally, anastomosis of the pre-implantation network with host vessels occurs. Anastomosis between HUVEC-derived vessels and host (mouse) vessels has been detected (46) and this occurs as early as 1 day after implantation (18), although it is not clear to what extent anastomosis occurs. Whether our prevascularized BAMs survive *in vivo* and allow for anastomosis will be assessed by future implantation experiments.

We also tested the addition of 10% Matrigel in coculture BAMs. Matrigel has been used in combination with collagen type I to form BAMs (19). It is a gelatinous protein mixture obtained from mouse sarcoma cells containing many ECM-proteins and growth factors. Fibrin (1 mg/ml) without Matrigel supports a homogenous formation of myofibers. In contrast, in the BAMs with 10% Matrigel, the myofibers in the exterior 20 µm of the BAM are longer than in the condition without Matrigel. In the center of the BAM, the myofibers are less well aligned compared to the fibrin-only ECM. To conclude, we do not suggest using Matrigel as part of the ECM of BAMs with a fibrin-based ECM, in order to obtain homogenously distributed and formed myofibers. Moreover, the composition of Matrigel is not fully characterized.

In addition, different gel formulations and gelation conditions can strongly influence fibrin biochemistry and ultrastructure, which in turn has an important effect on its angiogenic properties and on cell behavior (47). Fibrin ultrastructure (and cell behavior) is also affected by fibrinogen and thrombin concentrations, calcium ion content, ionic strength, temperature, and pH during gelation. For both thrombin and fibrinogen, there is not only a difference between brands, but also within one brand depending on the source of the fibrin (47). Therefore, a direct comparison of these results with previous results in literature is difficult, since different research groups not only use different types of fibrin, but also different cell types, cell numbers and volumes of ECM in tissue engineering of BAMs (5,7,9,12,18–20).

In order to create muscle tissue similar to that in the adult body, still other hurdles need to be overcome. A major one is the formation of neuromuscular synapses. Therefore, myofibers should express functional nicotinic acetylcholine receptors (AchR) capable of generating acetylcholine induced action potentials. Acetylcholine receptor expression increases sharply just before myoblast fusion (48), but is distributed randomly along the surface. During later phases of myogenesis, these receptors cluster at the motor endplates. In the absence of neural cells, BAMs have been shown to form mature AchR clusters by the addition of agrin and laminin (49). In the absence of mature AchR clusters, BAMs can still be stimulated by electrical current, which results in increased protein synthesis, increased force production and excitability (5,50). The introduction of neural cells to a monolayer of myotubes resulted in the formation of neuromuscular-like junctions with clustering of acetylcholine receptors (51). It is not known whether endothelial cells could affect the expression of muscle nicotinic receptors and/or induce clustering of AchR. This could be further studied with our coculture system. Furthermore, BAMs should remain under tension *in vivo* in order to avoid atrophy. Therefore, another issue to be addressed is the integration of BAMs with (bio-artificial) tendons. Our model system allows for extensive biochemical, physical, cellular and electrical characterization of the effect of adding different cell types to muscle cells during myofiber formation. It thus bridges the gap between 2D culture systems and *in vivo* transplantation of exogenous muscle tissue.

To our knowledge, we have tissue engineered for the first time a human bio-artificial muscle containing advanced endothelial cell networks by coculturing HUVECs and human muscle cells in a fibrin ECM.

Acknowledgements

The authors thank Petra D'hooge for technical assistance with confocal microscopy and Sigrid Vanryckeghem for administrative support. This work was funded by the Research Fund KU Leuven (CREA/12/034). LT is a Postdoctoral Fellow of the Research Foundation-Flanders (FWO).

Author disclosure statement

No competing financial interests exist

References

1. Hinds S, Bian W, Dennis RG, Bursac N. The role of extracellular matrix composition in structure and function of bioengineered skeletal muscle. Biomaterials. **32**(14), 3575, 2011;

2. Fishman JM, Tyraskis A, Maghsoudlou P, Urbani L, Totonelli G, Birchall M, et al. Skeletal Muscle Tissue Engineering: Which Cell to Use? Tissue Eng. Part B. Rev. **44**(6), 1, 2013;

3. Klumpp D, Horch RE, Beier JP. Tissue engineering of skeletal muscle. Tissue Eng. tissue organ Regen. intechopen; 2011.

4. Thorrez L, Shansky J, Wang L, Fast L, VandenDriessche T, Chuah M, et al. Growth, differentiation, transplantation and survival of human skeletal myofibers on biodegradable scaffolds. Biomaterials. **29**(1), 75, 2008;

5. Vandenburgh H, Shansky J, Benesch-Lee F, Barbata V, Reid J, Thorrez L, et al. Drug-screening platform based on the contractility of tissue-engineered muscle. Muscle Nerve. **37**(4), 438, 2008;

6. Shansky J, Chromiak J. A simplified method for tissue engineering skeletal muscle organoids in vitro. In Vitro Cell. Dev. Biol. Anim. **33**(5), 659, 1997;

7. Levenberg S, Rouwkema J, Macdonald M, Garfein ES, Kohane DS, Darland DC, et al. Engineering vascularized skeletal muscle tissue. Nat. Biotechnol. **23**(7), 879, 2005;

8. Shandalov Y, Egozi D, Koffler J, Dado-Rosenfeld D, Ben-Shimol D, Freiman A, et al. An engineered muscle flap for reconstruction of large soft tissue defects. Proc. Natl. Acad. Sci. U. S. A. **111**(16), 6010, 2014;

9. Lesman A, Koffler J, Atlas R, Blinder YJ, Kam Z, Levenberg S. Engineering vessel-like networks within multicellular fibrin-based constructs. Biomaterials. **32**(31), 7856, 2011;

10. Nagamori E, Ngo TX, Takezawa Y, Saito A, Sawa Y, Shimizu T, et al. Network formation through active migration of human vascular endothelial cells in a multilayered skeletal myoblast sheet. Biomaterials. **34**(3), 662, 2013;

11. Carosio S, Barberi L, Rizzuto E, Nicoletti C, Prete Z Del, Musarò A. Generation of eX vivo-vascularized Muscle Engineered Tissue (X-MET). Sci. Rep. **3**, 1420, 2013;

12. Criswell TL, Corona BT, Wang Z, Zhou Y, Niu G, Xu Y, et al. The role of endothelial cells in myofiber differentiation and the vascularization and innervation of bioengineered muscle tissue in vivo. Biomaterials. Elsevier Ltd; 1, 2012;

13. Miller JS, Stevens KR, Yang MT, Baker BM, Nguyen D-HT, Cohen DM, et al. Rapid casting of patterned vascular networks for perfusable engineered three-dimensional tissues. Nat. Mater. **11**(7), 1, 2012;

14. Van der Schaft DWJ, van Spreeuwel ACC, van Assen HC, Baaijens FPT. Mechanoregulation of vascularization in aligned tissue-engineered muscle: a role for vascular endothelial growth factor. Tissue Eng. Part A. **17**(21-22), 2857, 2011;

15. Juhas M, Engelmayr GC, Fontanella AN, Palmer GM, Bursac N. Biomimetic engineered muscle with capacity for vascular integration and functional maturation in vivo. Proc. Natl. Acad. Sci. U. S. A. **111**(15), 5508, 2014;

16. Rasband W. ImageJ. U. S. National Institutes of Health, Bethesda, Maryland, USA: http://imagej.nih.gov/ij/;

17. Carpentier G. Angiogenesis Analyzer for ImageJ - Gilles Carpentier Research Web Site: Computer Image Analysis. 2012.

18. Koffler J, Kaufman-Francis K, Yulia S, Dana E, Daria AP, Landesberg A, et al. Improved vascular organization enhances functional integration of engineered skeletal muscle grafts. Proc. Natl. Acad. Sci. U. S. A. **108**(36), 14789, 2011;

19. Thorrez L, Vandenburgh H, Callewaert N, Mertens N, Shansky J, Wang L, et al. Angiogenesis enhances factor IX delivery and persistence from retrievable human bioengineered muscle implants. Mol. Ther. **14**(3), 442, 2006;

20. Rosso F, Marino G, Giordano A, Barbarisi M, Parmeggiani D, Barbarisi A. Smart materials as scaffolds for tissue engineering. J. Cell. Physiol. **203**(3), 465, 2005;

21. Morin KT, Tranquillo RT. Guided sprouting from endothelial spheroids in fibrin gels aligned by magnetic fields and cell-induced gel compaction. Biomaterials. **32**(26), 6111, 2011;

22. Morin KT, Smith AO, Davis GE, Tranquillo RT. Aligned human microvessels formed in 3D fibrin gel by constraint of gel contraction. Microvasc. Res. **90**, 12, 2013;

23. Morin KT, Dries-Devlin JL, Tranquillo RT. Engineered Microvessels with Strong Alignment and High Lumen Density Via Cell-Induced Fibrin Gel Compaction and Interstitial Flow. Tissue Eng. Part A. **20**, 2013;

24. Chiron S, Tomczak C, Duperray A, Lainé J, Bonne G, Eder A, et al. Complex interactions between human myoblasts and the surrounding 3D fibrin-based matrix. PLoS One. **7**(4), e36173, 2012;

25. Nakatsu MN, Sainson RCA, Aoto JN, Taylor KL, Aitkenhead M, Pérez-del-Pulgar S, et al. Angiogenic sprouting and capillary lumen formation modeled by human umbilical vein endothelial cells (HUVEC) in fibrin gels: the role of fibroblasts and Angiopoietin-1. Microvasc. Res. **66**(2), 102, 2003;

26. Arnaoutova I, George J, Kleinman HK, Benton G. The endothelial cell tube formation assay on basement membrane turns 20: State of the science and the art. Angiogenesis. **12**, 267, 2009;

27. Baldwin J, Antille M, Bonda U, De-Juan-Pardo EM, Khosrotehrani K, Ivanovski S, et al. In vitro pre-vascularisation of tissue-engineered constructs A co-culture perspective. Vasc. Cell. **6**, 13, 2014;

28. Sahni A, Francis CW. Vascular endothelial growth factor binds to fibrinogen and fibrin and stimulates endothelial cell proliferation. Blood. **96**(12), 3772, 2000;

29. Engler AJ, Griffin M a, Sen S, Bönnemann CG, Sweeney HL, Discher DE. Myotubes differentiate optimally on substrates with tissue-like stiffness: pathological implications for soft or stiff microenvironments. J. Cell Biol. **166**(6), 877, 2004;

30. Hinds S, Bian W, Dennis RG, Bursac N. The role of extracellular matrix composition in structure and function of bioengineered skeletal muscle. Biomaterials. Elsevier Ltd; **32**(14), 3575, 2011;

31. Martin NRW, Passey SL, Player DJ, Khodabukus A, Ferguson R a, Sharples AP, et al. Factors affecting the structure and maturation of human tissue engineered skeletal muscle. Biomaterials. Elsevier Ltd; **34**(23), 5759, 2013;

32. Cassano M, Biressi S, Finan A, Benedetti L, Omes C, Boratto R, et al. Magic-factor 1, a partial agonist of Met, induces muscle hypertrophy by protecting myogenic progenitors from apoptosis. PLoS One. **3**(9), e3223, 2008;

33. Powell C a, Smiley BL, Mills J, Vandenburgh HH. Mechanical stimulation improves tissue-engineered human skeletal muscle. Am. J. Physiol. Cell Physiol. **283**(5), C1557, 2002;

34. Rangarajan S, Madden L, Bursac N. Use of Flow, Electrical, and Mechanical Stimulation to Promote Engineering of Striated Muscles. Ann. Biomed. Eng. 2013;

35. Van Beem RT, Verloop RE, Kleijer M, Noort W a, Loof N, Koolwijk P, et al. Blood outgrowth endothelial cells from cord blood and peripheral blood: angiogenesis-related characteristics in vitro. J. Thromb. Haemost. **7**(1), 217, 2009;

36. Yoder MC, Mead LE, Prater D, Krier TR, Mroueh KN, Li F, et al. Redefining endothelial progenitor cells via clonal analysis and hematopoietic stem/progenitor cell principals. Blood. **109**(5), 1801, 2007;

37. Melero-Martin JM, Khan Z a., Picard A, Wu X, Paruchuri S, Bischoff J. In vivo vasculogenic potential of human blood-derived endothelial progenitor cells. Blood. **109**(11), 4761, 2007;

38. Au P, Daheron LM, Duda DG, Cohen KS, Tyrrell J a, Lanning RM, et al. Differential in vivo potential of endothelial progenitor cells from human umbilical cord blood and adult peripheral blood to form functional long-lasting vessels. Blood. **111**(3), 1302, 2008;

39. Kunz-Schughart L a, Schroeder J a, Wondrak M, van Rey F, Lehle K, Hofstaedter F, et al. Potential of fibroblasts to regulate the formation of three-dimensional vessel-like structures from endothelial cells in vitro. Am. J. Physiol. Cell Physiol. **290**, C1385, 2006;

40. Sampaolesi M, Blot S, D'Antona G, Granger N, Tonlorenzi R, Innocenzi A, et al. Mesoangioblast stem cells ameliorate muscle function in dystrophic dogs. Nature. **444**(7119), 574, 2006;

41. Hanjaya-Putra D, Shen Y-I, Wilson A, Fox-Talbot K, Khetan S, Burdick JA, et al. Integration and regression of implanted engineered human vascular networks during deep wound healing. Stem Cells Transl. Med. **2**(4), 297, 2013;

42. Roh JD, Sawh-Martinez R, Brennan MP, Jay SM, Devine L, Rao DA, et al. Tissue-engineered vascular grafts transform into mature blood vessels via an inflammation-mediated process of vascular remodeling. Proc. Natl. Acad. Sci. U. S. A. **107**(10), 4669, 2010;

43. Vandenburgh H, Shansky J, Benesch-Lee F, Skelly K, Spinazzola JM, Saponjian Y, et al. Automated drug screening with contractile muscle tissue engineered from dystrophic myoblasts. FASEB J. **23**(10), 3325, 2009;

44. Vandenburgh H. High-content drug screening with engineered musculoskeletal tissues. Tissue Eng. Part B. Rev. **16**(1), 55, 2010;

45. Juhas M, Engelmayr GC, Fontanella a. N, Palmer GM, Bursac N. Biomimetic engineered musde with capacity for vascular integration and functional maturation in vivo. Proc. Natl. Acad. Sci. 1, 2014;

46. Shandalov Y, Egozi D, Koffler J, Dado-Rosenfeld D, Ben-Shimol D, Freiman A, et al. An engineered muscle flap for reconstruction of large soft tissue defects. Proc. Natl. Acad. Sci. U. S. A. 2, 2014;

47. Morin KT, Tranquillo RT. In vitro models of angiogenesis and vasculogenesis in fibrin gel. Exp. Cell Res. **319**(16), 2409, 2013;

48. Krause RM, Hamann M, Bader CR, Liu JH, Baroffio a, Bernheim L. Activation of nicotinic acetylcholine receptors increases the rate of fusion of cultured human myoblasts. J. Physiol. **489**(3), 779, 1995;

49. Wang L, Shansky J, Vandenburgh H. Induced formation and maturation of acetylcholine receptor clusters in a defined 3D bio-artificial muscle. Mol. Neurobiol. **48**(3), 397, 2013;

50. Donnelly K, Khodabukus A, Philp A, Deldicque L, Dennis RG, Baar K. A novel bioreactor for stimulating skeletal muscle in vitro. Tissue Eng. Part C. Methods. **16**(4), 711, 2010;

51. Larkin LM, Van der Meulen JH, Dennis RG, Kennedy JB. Functional evaluation of nerve -skeletal muscle constructs engineered in vitro. In Vitro Cell. Dev. Biol. Anim. **42**(3-4), 75, 2007;

Figure legends

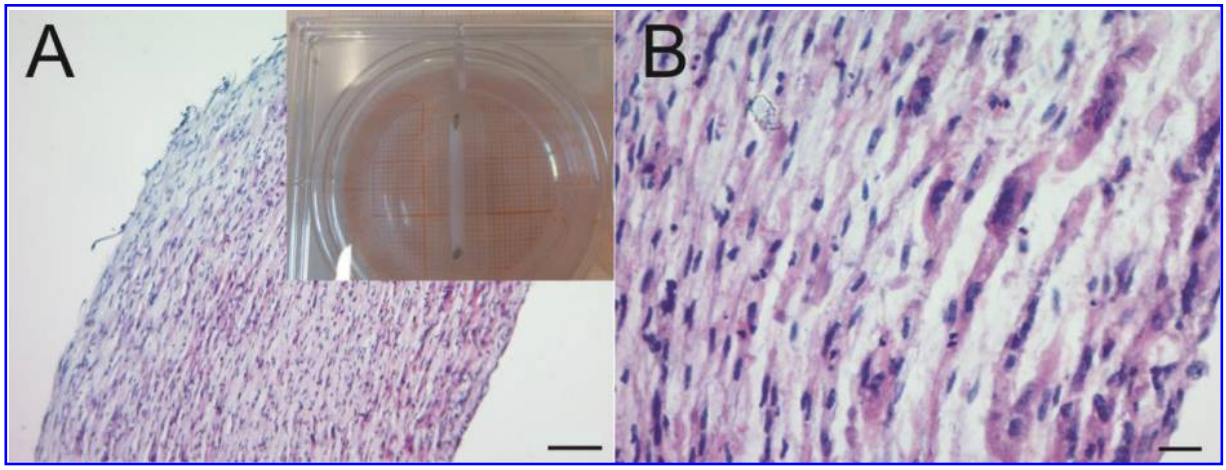

Figure 1. H&E staining of a bio-artificial muscle (BAM) with 1.10^6 muscle cells in a fibrin extracellular matrix shown with a 10x (A) and 40x (B) objective. Inset shows a seven-day old BAM in a 6-well plate, fixed to two attachment sites which are 2 cm apart. Myofibers are aligned and homogenously distributed over the entire BAM. Scale bars represent 50 (A) and 10 µm (B).

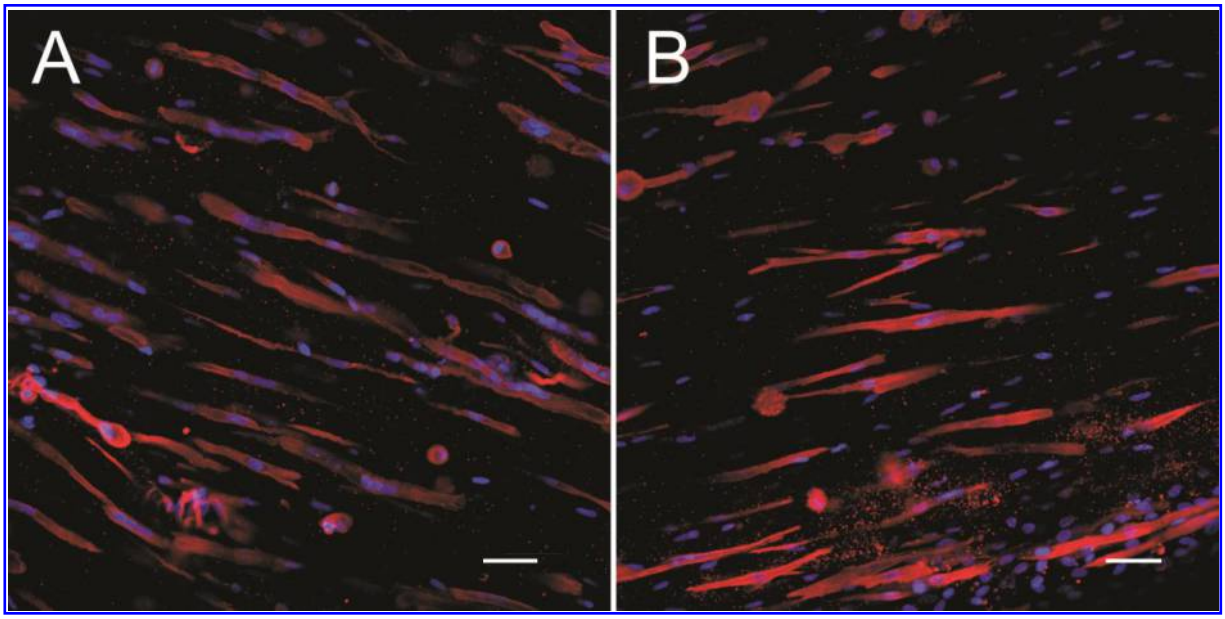

Figure 2. Multinucleated myofibers in BAMs with 1.10^6 muscle cells, cultured in (A) SkGM-SkFM and (B) EGM-2 medium. Blue: nuclei stained with DAPI; red: myofibers stained with tropomyosin immunofluorescence.

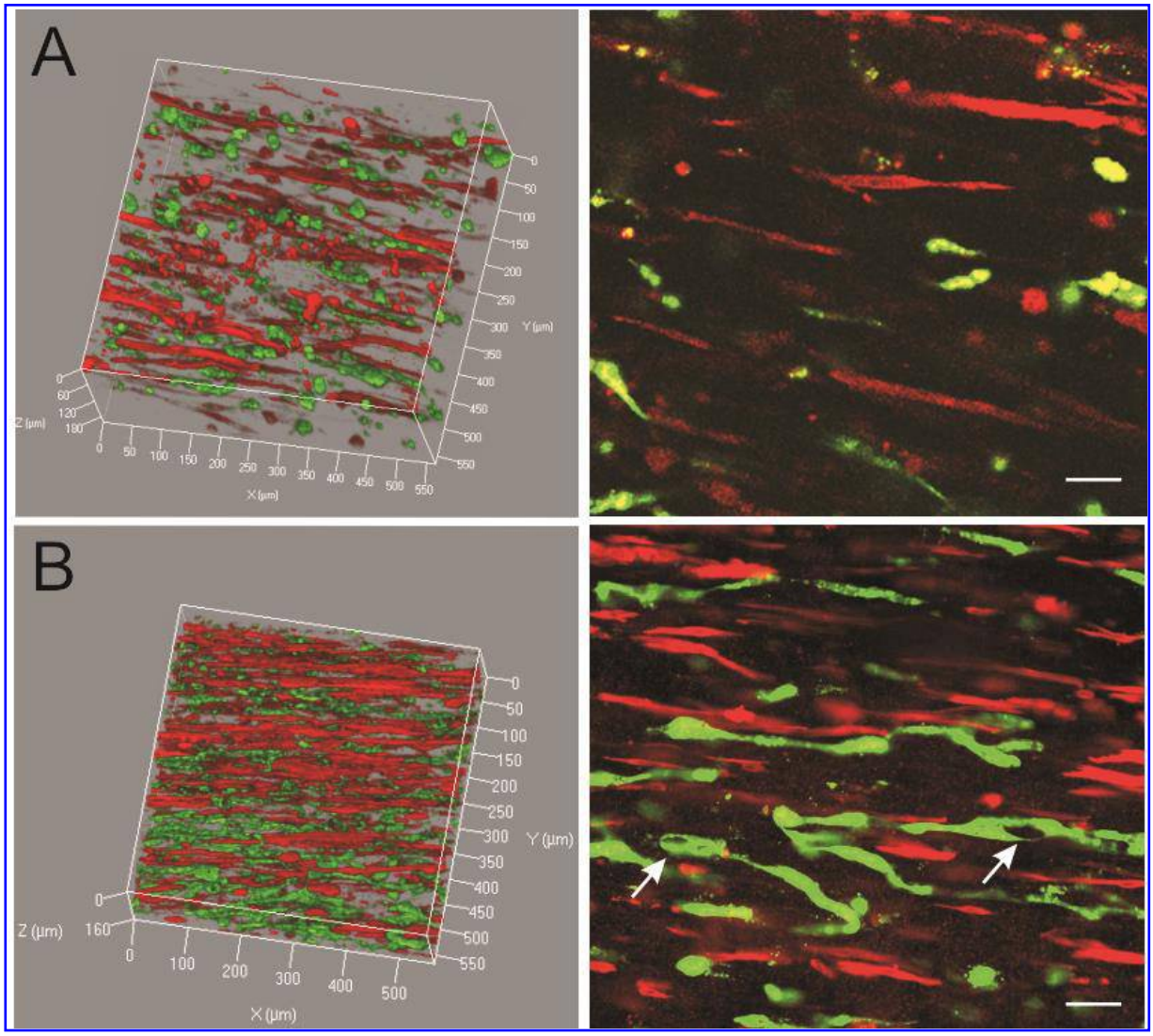

Figure 3. Fluorescent confocal images of coculture BAM with 50% HUVECs and 50% muscle cells and a total cell number of 1.10^6 cells (A) and 2.10^6 cells (B). Endothelial networks (green) between aligned myofibers (red) in 3D (left) and an xy-cross section in 2D (right). Scale bars represent 50 µm, meshes are indicated by arrows.

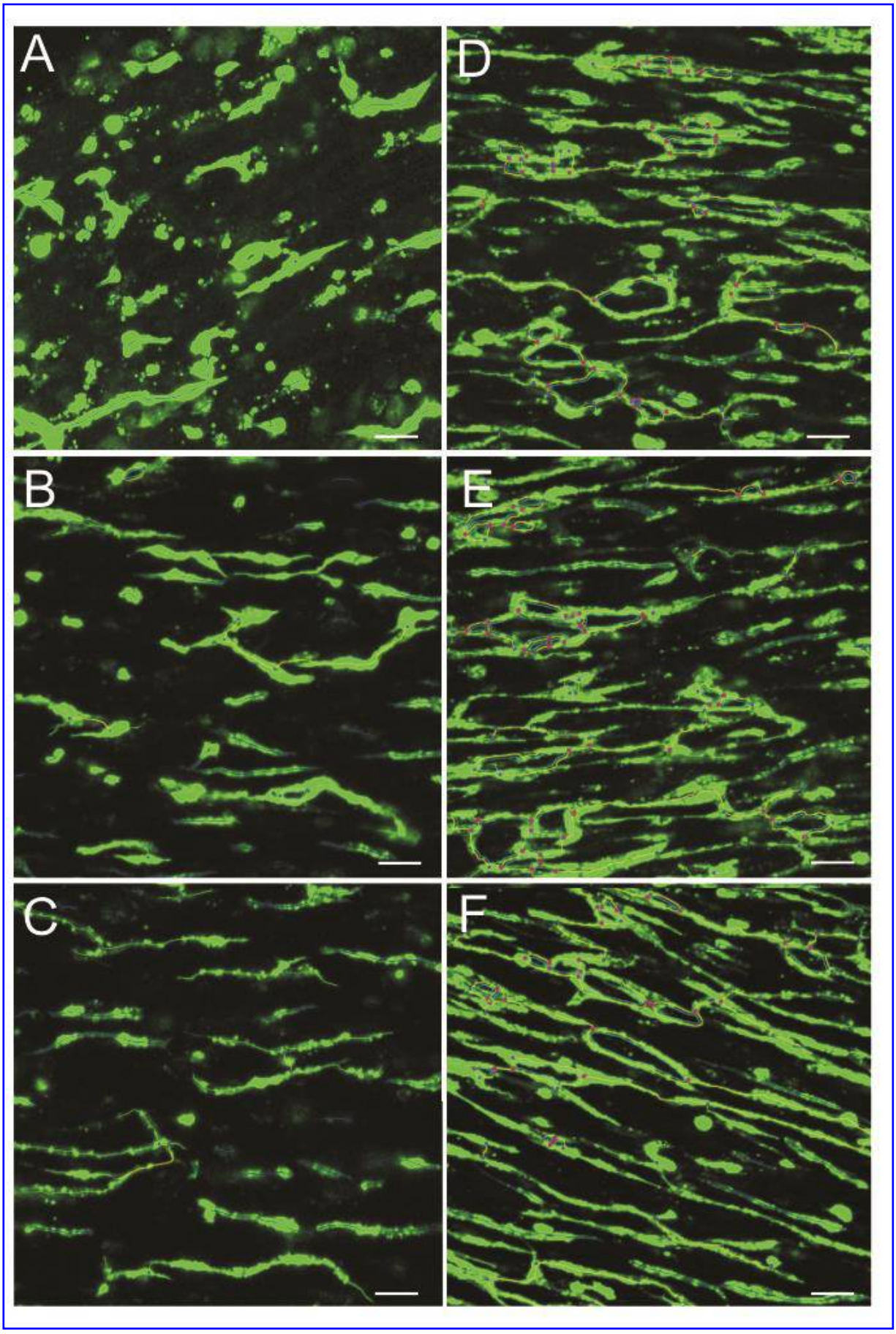

Figure 4. (A) Analysis by Angiogenesis Analyzer ImageJ's plugin, visualizing endothelial network formation of 60 µm z-projection images of fibrin BAMs with a total of 1.10^6 cells with 50% (A), 40% (B) and 30% (C) HUVECs or with a total of 2.10^6 cells with 50% (D), 40% (E) and 30% (F) HUVECs. Angiogenesis Analyzer indicates master junctions (pink dots), master segments (yellow), meshes (light blue), branches (green) and isolated segments (blue). Scale bar represents 50 µm.

Table legends

Table 1. Myofiber formation in fibrin BAMs with only muscle cells (5.10^6 or 1.10^6 cells) or coculture BAMs with 50% HUVECs and 1.10^6 or 2.10^6 cells in total, cultured in SkGM-SkFM (column A) or EGM-2 medium (columns B-G) for 7 days. Columns A–E are discussed and compared in section 3.1, columns F– G are discussed in section 3.4. In the last 7 columns, statistical significances are shown for comparisons of indicated groups. Multiple comparisons were made by a Kruskal Wallis test followed by a Dunn's post test except for the parameter diameter where a parametric ANOVA followed by a Bonferroni post test was used.

Table 2. Thickness (in mm) of different fibrin BAMs, cultured for 7 days in EGM-2 medium. In section 3.2, only column A is discussed. In section 3.4, a comparison is made between column A and B.

Table 3. Parameters characterizing the formation of endothelial networks in fibrin coculture BAMs with a total of 1.10^6 cells with 50% (A), 40% (B) and 30% (C) HUVECs or with a total of 2.10^6 cells with 50% (D), 40% (E) and 30% (F) HUVECs .In the last 5 columns, statistical significances are shown for comparisons of indicated groups. Comparisons B-C, D-E, D-F and E-F were also made but did not result in statistically significant differences for any of the parameters. For multiple comparisons within groups (1.10^6 total cell count (A, B and C) or 2.10^6 total cell count (D, E and F)), a nonparametric Kruskal-Wallis test with Dunn's post test was used. For pairwise comparisons between groups (A-D, B-E and C-F), a Mann Whitney test was performed.

Table 4. Parameters characterizing the formation of myofibers in fibrin coculture BAMs with a total of 1.10^6 cells with 50% (A), 40% (B) and 30% (C) HUVECs or with a total of 2.10^6 cells with 50% (D), 40% (E) and 30% (F) HUVECs. In the last 9 columns, statistical significances are shown for comparisons of indicated groups. For multiple comparisons within groups (1.10^6 total cell count (A, B and C) or 2.10^6 total cell count (D, E and F)), a nonparametric Kruskal-Wallis test with Dunn's post test was used. For pairwise comparisons between groups (A-D, B-E and C-F), a Mann Whitney test was performed.

Table 1

	A (n=12)	**B (n=8)**	**C (n=11)**	**D (n=10)**	**E (n=34)**	**F (n=11)**	**G (n=75)**	**A-D**	**B-C**	**D-E**	**C-E**	**B-D**	**D-F**	**D-G**
# Myoblasts	**1.10^6**	**5.10^5**	**5.10^5**	**1.10^6**	**1.10^6**	**1.10^6**	**1.10^6**							
# HUVECs	**0**	**0**	**5.10^5**	**0**	**1.10^6**	**0**	**0**							
Medium	**SkGM/SkFM**	**EGM-2**	**EGM-2**	**EGM-2**	**EGM-2**	**EGM-2**	**EGM-2**							
						+10% matrigel outer 20 µm	**+10% matrigel inner 140 µm**							
Number/microscopic field	42.20 ± 7.64	21.51 ± 2.34	25.63 ± 10.02	39.96 ± 5.75	40.48 ± 10.25	37.09 ± 17.14	35.21 ± 8.24	NS	NS	NS	**	*	NS	NS
Alignment	10.34 ± 4.95	11.36 ± 4.00	16.24 ± 5.96	8.04 ± 1.89	5.09 ± 1.33	7.51 ± 3.76	14.07 ± 4.45	NS	NS	NS	***	NS	NS	***
Length (µm)	147.60 ± 14.11	118.7 ± 16.30	118.90 ± 6.93	126.30 ± 7.02	127.4 ± 37.56	176.30 ± 52.45	113.40 ± 21.21	NS	NS	NS	NS	NS	***	NS
Diameter (µm)	15.34 ± 3.78	10.81 ± 4.26	12.79 ± 4.60	12.20 ± 3.00	13.26 ± 3.69	14.27 ± 3.22	13.75 ± 3.67	*	NS	NS	NS	NS	NS	NS

Table 2

	A. Fibrin ECM	**B. Fibrin + 10% matrigel ECM**
5.10^5 muscle cells	3.20 ± 0.07 (n=3)	3.23 ± 0.35 (n=3)
1.10^6 muscle cells	2.48 ± 0.39 (n=3)	3.32 ±0.13 (n=3)
5.10^5 muscle cells + 5.10^5 GFP-HUVECs	2.20 ± 0.36 (n=3)	2.20 ±0.18 (n=3)
1.10^6 muscle cells + 1.10^6 GFP-HUVECs	1.27 ± 0.22 (n=12)	ND
12.10^5 muscle cells + 8.10^5 GFP HUVECs	1.30 ± 0.03 (n=4)	ND
14.10^5 muscle cells + 6.10^5 GFP HUVECs	1.28 ± 0.21 (n=4)	ND

Table 3

	A (n=37)	B (n=8)	C (n=5)	D (n=219)	E (n=65)	F (n=50)	A-B	A-C	A-D	B-E	C-F
Total # cells in BAM	**1.10^6**	**1.10^6**	**1.10^6**	**2.10^6**	**2.10^6**	**2.10^6**					
# Muscle cells	**5.10^5**	**6.10^5**	**7.10^5**	**10.10^5**	**12.10^5**	**14.10^5**					
# HUVECs	**5.10^5**	**4.10^5**	**3.10^5**	**10.10^5**	**8.10^5**	**6.10^5**					
% branching length	20.96 ± 13.28	39.05 ± 15.67	48.29 ± 8.19	76.36 ± 11.84	79.21 ± 8.01	75.92 ± 11.05	**	***	***	***	***
Number of isolated segments	51.24 ± 14.29	36.00 ± 8.40	29.60 ± 2.70	18.72 ± 9.89	15.37 ± 4.78	16.44 ± 5.41	**	***	***	***	***
Number of junctions	3.62 ± 2.64	7.63 ± 4.03	8.60 ± 2.61	47.43 ± 21.61	50.13 ± 13.54	49.64 ± 28.78	**	**	***	***	***
Number of branches	7.78 ± 4.92	15.13 ± 6.47	15.40 ± 5.37	45.96 ± 13.84	48.33 ± 9.68	46.14 ± 17.55	**	**	***	***	***
Total length (µm)	16422 µm ± 3591	20349 µm ± 5295	21488 ± 4574	38262 µm ± 7147	39920 µm ± 4942	40165 ± 8298	*	*	***	***	***
Number of meshes	0.49 ± 0.8035	0.75 ± 0.71	1.00 ± 0.70	10.50 ± 7.14	12.35 ± 5.182	12.38 ± 8.82	NS	NS	***	***	***

Table 4

	A (n=11)	**B (n=24)**	**C (n=19)**	**D (n=34)**	**E (n=20)**	**F (n=15)**	**A-B**	**A-C**	**B-C**	**D-E**	**D-F**	**E-F**	**A-D**	**B-E**	**C-F**
Total # cells in BAM	**1.10^6**	**1.10^6**	**1.10^6**	**2.10^6**	**2.10^6**	**2.10^6**									
# Muscle cells	**5.10^5**	**6.10^5**	**7.10^5**	**10.10^5**	**12.10^5**	**14.10^5**									
# HUVECs	**5.10^5**	**4.10^5**	**3.10^5**	**10.10^5**	**8.10^5**	**6.10^5**									
Number/ microscopic field	25.63 ±10.02	47.08 ±15.41	48.68 ± 12.56	40.48 ± 10.25	48.29 ± 13.62	49.16 ± 7.26	**	***	NS	NS	**	NS	**	NS	NS
Alignment	16.24 ± 5.96	6.25 ± 0.84	7.72 ± 4.30	5.09 ± 1.33	3.65 ± 0.79	4.912 ± 1.12	***	*	NS	***	NS	**	***	***	***
Length (µm)	118.90 ± 6.93	123.4 ± 13.9	119.7 ± 15.9	127.4 ± 37.56	121.3 ± 15.37	119.2 ± 13.18	NS	NS	NS	NS	NS	NS	NS	NS	NS
Diameter (µm)	12.79 ± 4.60	16.88 ± 8.82	24.05 ± 7.18	13.26 ± 3.69	12.22 ± 2.88	11.96 ± 1.058	NS	***	**	NS	NS	NS	NS	*	***

Supplemental information

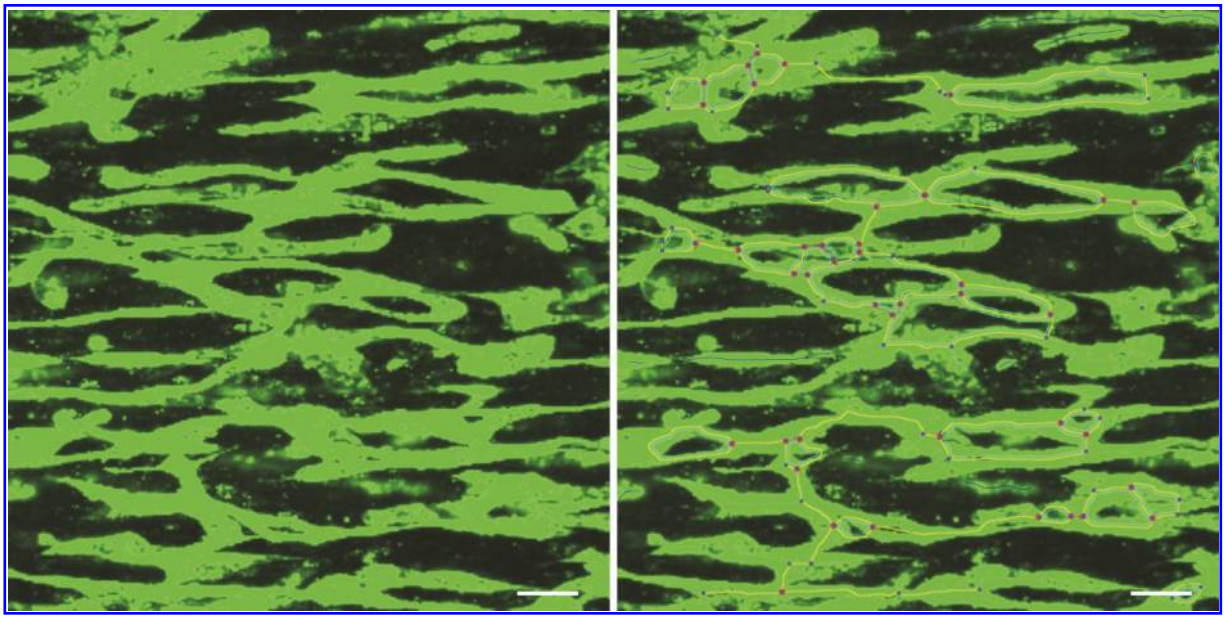

Figure S1. Quantification by Angiogenesis Analyzer (right) and original image (left) of endothelial network formation in a coculture BAM. In the right image, there is an indication of master junctions (pink dots), master segments (yellow), meshes (light blue), branches (green) and isolated segments (blue). Scale bar indicates 50 µm.

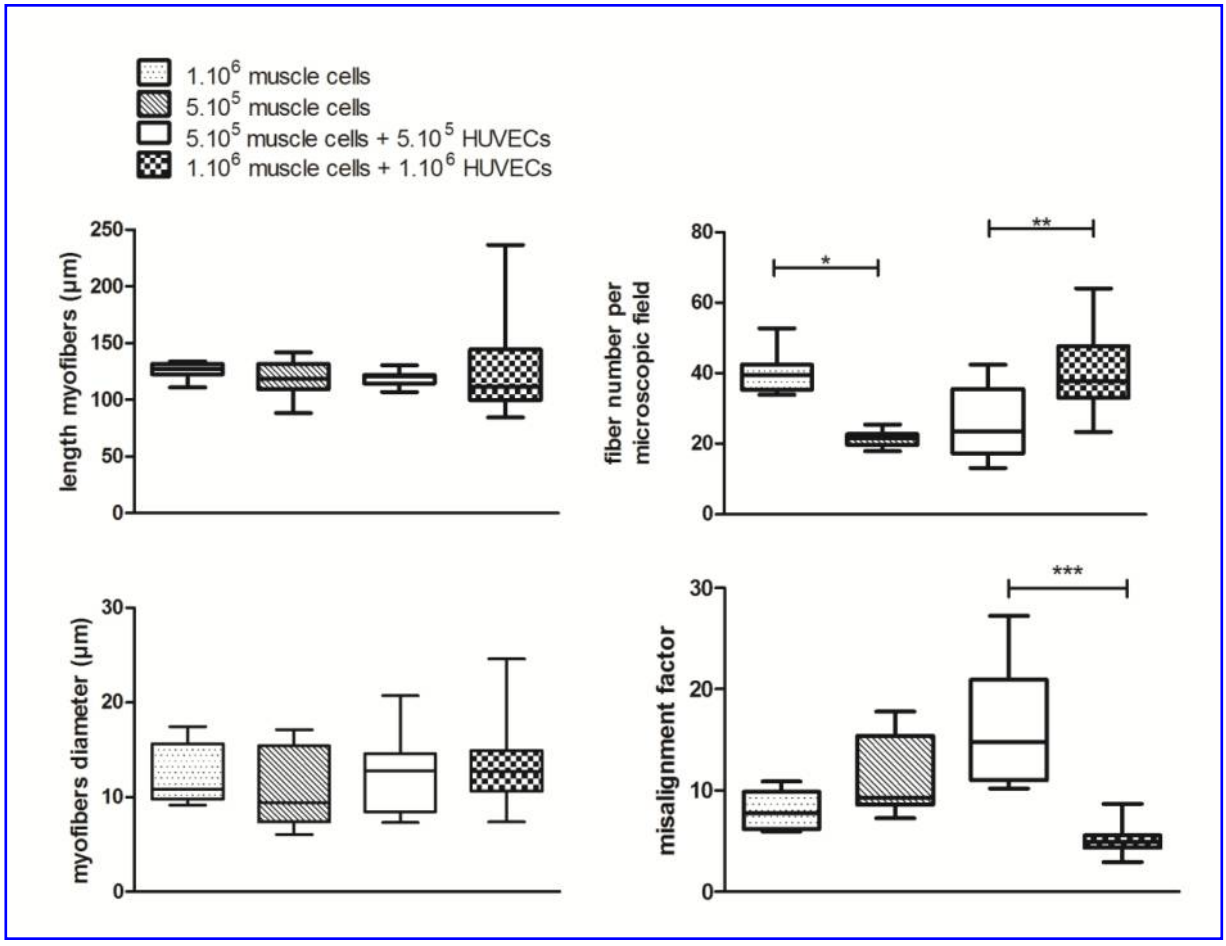

Figure S2. Myofiber formation in fibrin BAMs with 0.5 or 1.10^6 muscle cells with or without 0.5 or 1.10^6 HUVECs, respectively.

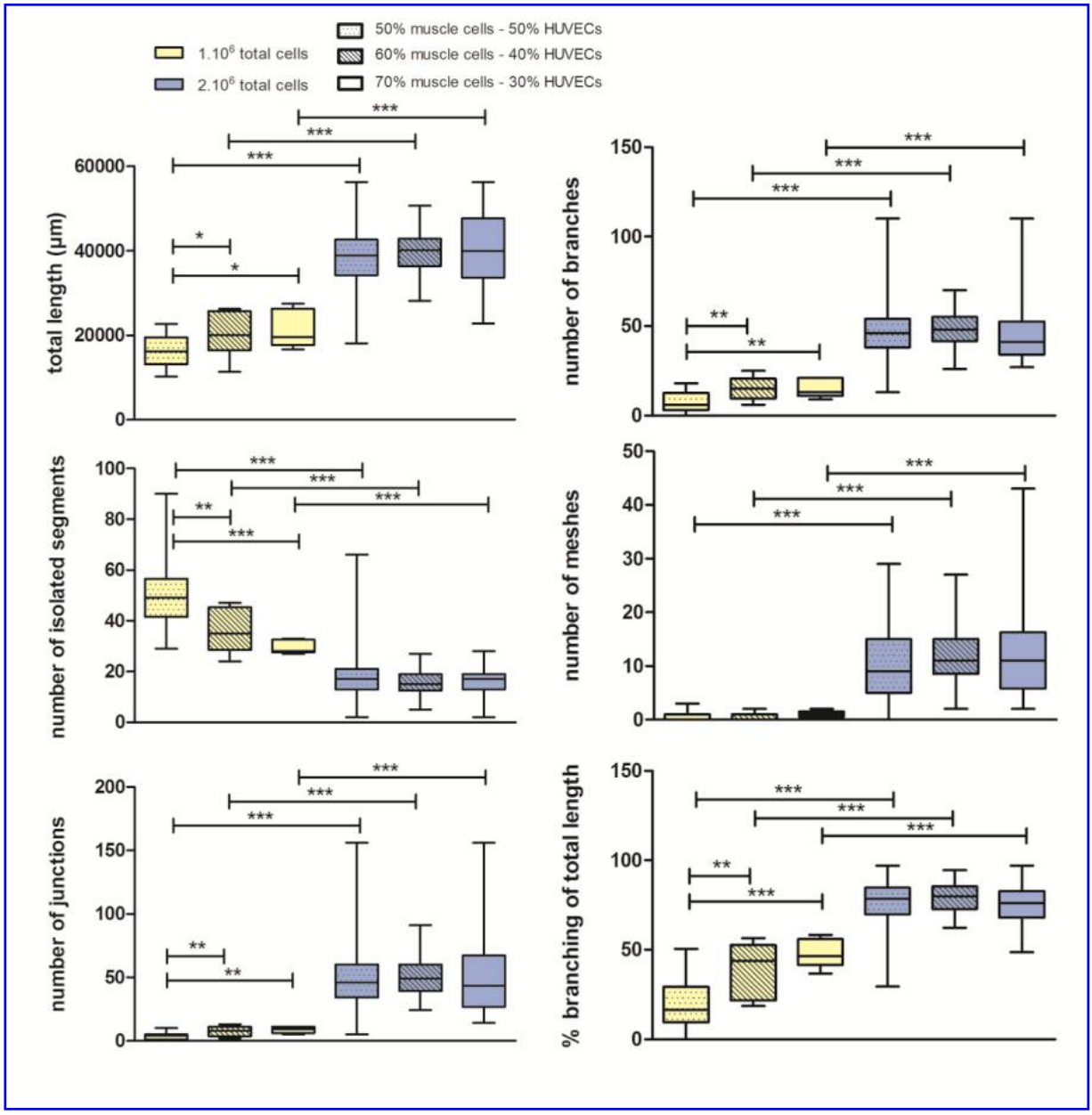

Figure S3. Endothelial network formation in coculture BAMs with different ratios of muscle cells and HUVECs in a total of 1.10^6 or 2.10^6 cells. This figure is a graphical representation of Table 3.

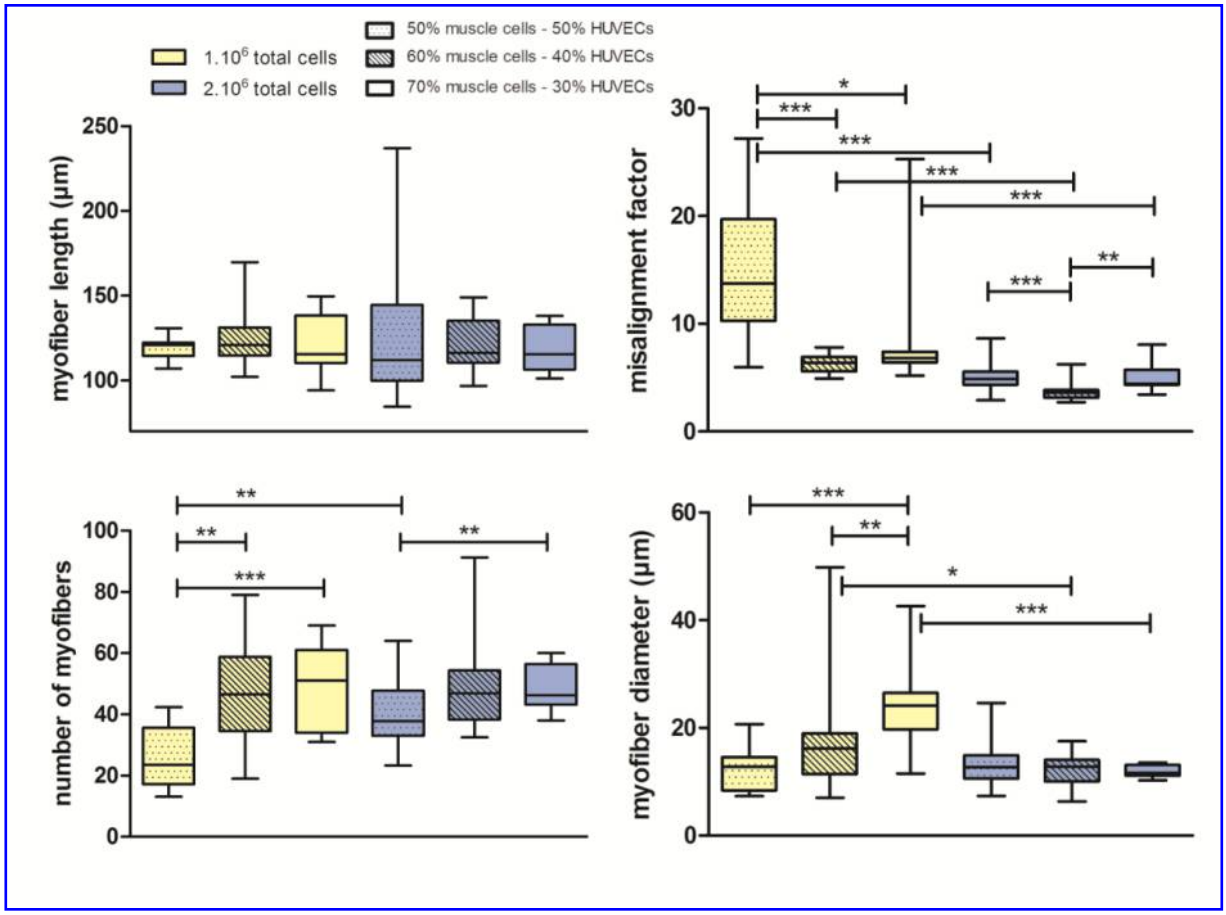

Figure S4. Myofiber formation in coculture BAMs with different ratios of muscle cells and HUVECs in a total of 1.10^6 or 2.10^6 cells. This figure is a graphical representation of Table 4.

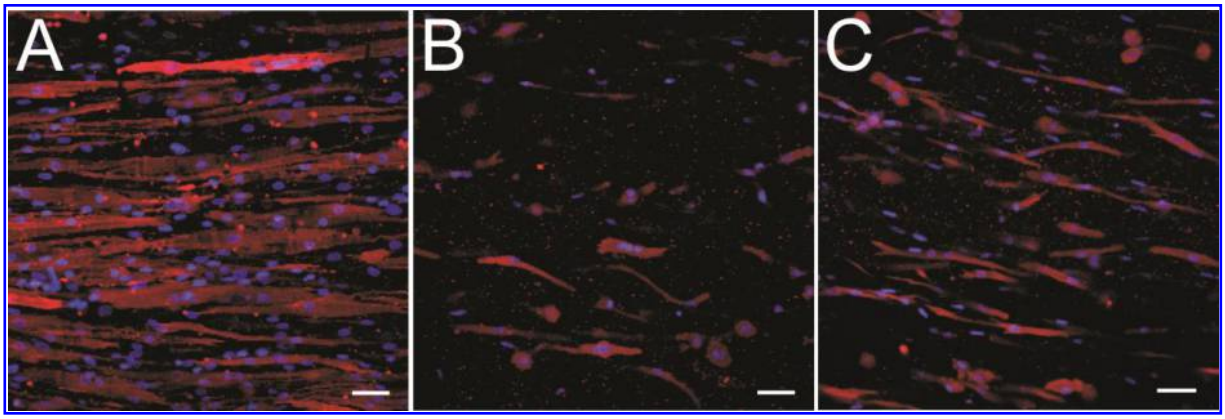

Figure S5. BAM with 1.10^6 muscle cells in an ECM of fibrin +10% matrigel (A and B show outer and inner zone respectively) and in a fibrin ECM without matrigel (C). The outer zone of 20 – 30 µm with matrigel (A) shows well aligned myofibers which are longer than in the condition without matrigel (C) whereas the inner zone (B) shows less well aligned myofibers compared to the condition shown in (C). Tropomyosin staining (red) shows myofibers, DAPI (blue) shows cell nuclei.

Video S1. Fluorescent confocal z-stack of aligned myofibers in coculture BAM with 50% HUVECs and 50% muscle cells and a total cell number of 2.10^6 cells. This video is a rotating 3D reconstruction of Figure 3B.

Video S2. Fluorescent confocal z-stack of endothelial networks in coculture BAM with 50% HUVECs and 50% muscle cells and a total cell number of 2.10^6 cells. This video is a rotating 3D reconstruction of Figure 3B.

Video S3. Fluorescent confocal z-stack of coculture BAM with 50% HUVECs and 50% muscle cells and a total cell number of 2.10^6 cells. Endothelial networks (green) between aligned myofibers (red) in 3D. This video is a rotating 3D reconstruction of Figure 3B.

gholobova.videos1.mp4

gholobova.videos2.mp4

gholobova.videos3.mp4